Click reaction as a useful tool to creatively combine pharmacophores: The case of Vismodegib

Michael S. Christodoulou[a], Mattia Mori[b], Rebecca Pantano[a], Romina Alfonsi[c], Paola Infante[b], Maurizio Botta[d,e], Giovanna Damia[f], Francesca Ricci[f], Panagiota A. Sotiropoulou[g], Sandra Liekens[h], Bruno Botta[i], Daniele Passarella[a,*]

[a] *Dipartimento di Chimica, Università degli Studi di Milano, Via Golgi 19, 20133 Milano, Italy*
[b] *Center for Life Nano Science@Sapienza, Istituto Italiano di Tecnologia, Viale Regina Elena 291, 00161 Roma, Italy*
[c] *Department of Molecular Medicine, University La Sapienza, 00161 Rome, Italy*
[d] *Dipartimento di Biotecnologie, Chimica e Farmacia, Università degli Studi di Siena, Via A. Moro 2, 53100 Siena, Italy*
[e] *Sbarro Institute for Cancer Research and Molecular Medicine, Center for Biotechnology, College of Science and Technology, Temple University, BioLife Science Bldg., Suite 333, 1900 N 12th Street, Philadelphia, PA 19122, USA*
[f] *Department of Oncology – IRCCS-Istituto di Ricerche Farmacologiche Mario Negri – Via La Masa 19 – 20156 Milano, Italy*
[g] *IRIBHM, Université Libre de Bruxelles, 808 Route de Lennik, 1070 Brussels, Belgium*
[h] *Rega Institute for Medical Research, KU Leuven, Minderbroedersstraat 10, blok x - bus 1030, B-3000 Leuven, Belgium*
[i] *Dipartimento di Chimica e Tecnologie del Farmaco, Università degli Studi di Roma "La Sapienza", Piazzale Aldo Moro 5, 00185 Roma, Italy*

[*]Corresponding author:
Tel.: +39 02.50314081; fax: +39 02.50314078; E-mail: daniele.passarella@unimi.it (D. Passarella).

Abstract: The design and the preparation of a small library of 1,4-diphenyl-1,2,3-triazole derivatives is reported, with the aim to obtain a new class of Hedgehog pathway inhibitors. The smoothened (SMO) protein is part of the hedgehog signalling pathway that is inhibited by the lead compound Vismodegib. Based on molecular modeling suggestions, seven triazole derivatives of Vismodegib were synthesized and their biological effect on different endothelial, cancer and cancer stem cell lines is reported.

Keywords: hedgehog pathway, click reaction, vismodegib, SMO protein, cancer stem cells.

1. Introduction

Vismodegib[1] is a synthetic Smoothened (SMO) antagonist that inhibits the Hedgehog (Hh) signaling pathway,[2] by preventing SMO translocation to the primary cilium. Acquired resistance to Vismodegib, due to smoothened mutations during the treatment of locally advanced basal cell carcinoma, has been reported recently.[3] The design of new scaffolds for the discovery of novel Hh inhibitors[4] is a current goal that could help to face the problem of cancer stem cells[5] whose behavior depends also on the Hedgehog pathway.[6] Therefore, we considered the modification of the Vismodegib scaffold to look for an improvement of its performance or to further explore its pharmacophoric properties.

Based on our previous results,[7, 8] we focused our attention on the substitution of the amide bond present in the Vismodegib structure with a 1,2,3-triazole ring. The bioisosterism between the amide group and 1,2,3-triazole ring is well known[9] and further supported herein by docking simulations. In this paper we report the rational design, versatile synthesis and biological evaluation of triazole-based Vismodegib analogues.
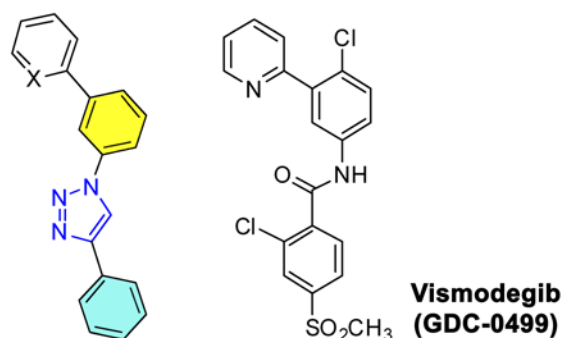

Figure 1. General structure of designed Vismodegib analogues.
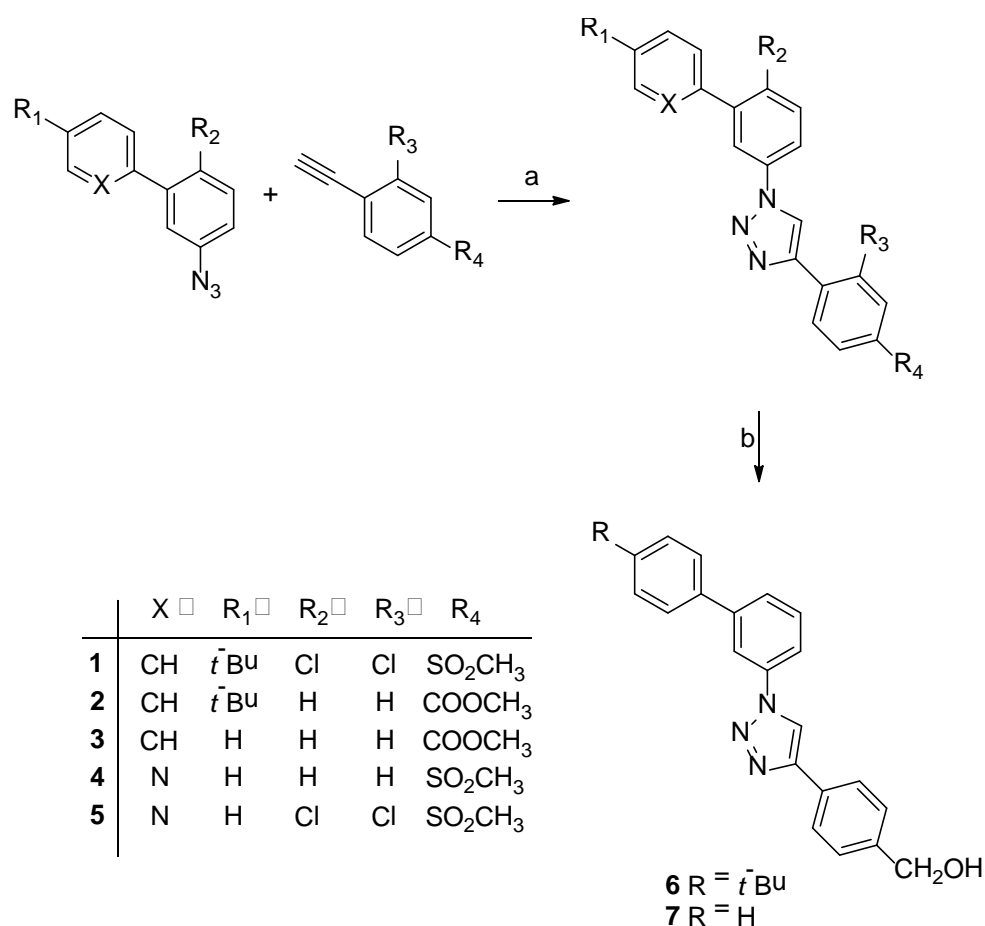
2. Results and Discussion

2.1. Molecular Modeling

A small virtual library of 140 triazole derivatives was built in silico as previously reported, based on the synthetic feasibility of the compounds and accounting for a number of simple and pharmacophoric substituents.[10]

To monitor whether amide replacement with triazole in Vismodegib scaffold may impact SMO binding, the virtual library of triazole derivatives and Vismodegib were docked within the antagonist site at the extracellular end of the SMO heptahelical bundle. To this aim, the crystallographic structure of SMO in complex with a small molecule antagonist (PDB ID: 4JKV)[11] was used as rigid receptor in molecular docking simulations, which were performed with the HYBRID program from OpenEye (see Materials and Methods for computational details).[12, 13] Due to the lack of benchmarking studies on the performance of docking and scoring functions to the SMO receptor, theoretical affinity was herein computed by the Chemgauss4 and the XSCORE functions.[14]

Based on results obtained by docking the virtual library, seven triazoles (**1**-**7**, Scheme 1) were synthesized as described in Scheme 1 and tested *in vitro.*

2.2. Chemistry

The synthesis of the final compounds **1** - **7** was accomplished according to the general synthetic strategy based on a 1,3-dipolar cycloaddition and reported in Scheme 1. The preparation of the proper building blocks is described in Scheme 2 (azides) and Scheme 3 (alkynes). A Suzuki coupling reaction of 4-*tert*-butylphenylboronic acid (Scheme 2) with 1-chloro-2-iodo-4-nitrobenzene (**9**) or the commercially available 1-iodo-3-nitrobenzene (**10**) provided the intermediates **11** and **12** in excellent yields. Continuously, reduction of the nitro group, with hydrazine monohydrate/iron(III) chloride in the presence of active carbon gave the amines **13** and **14**, which were then transformed to the azide derivatives **15** and **16** by the formation of diazonium salt and subsequent reaction with a solution of sodium azide in water. Sharpless cycloaddition[8] of azides **15** and **16** with alkynes **29** and the commercially available methyl 4-ethynylbenzoate furnished the desired products **1** and **2** respectively (65-75 % yield). Reduction of compound **2** with LiAlH$_4$ afforded the desired derivative **6**.

	X	R$_1$	R$_2$	R$_3$	R$_4$
1	CH	t-Bu	Cl	Cl	SO$_2$CH$_3$
2	CH	t-Bu	H	H	COOCH$_3$
3	CH	H	H	H	COOCH$_3$
4	N	H	H	H	SO$_2$CH$_3$
5	N	H	Cl	Cl	SO$_2$CH$_3$

6 R = t-Bu
7 R = H

Scheme 1. Reagents and conditions: (a) Corresponding azides and alkynes, sodium ascorbate, CuSO$_4$·5H$_2$O, t-BuOH:H$_2$O (1:1), reflux, 3 h; (b) LiAlH$_4$, THF, 0 °C to rt, 1 h.

Synthesis of the compound **3** was accomplished in a two-step sequence: the commercially available amine **24** was transformed to azide **25** and then submitted to a Sharpless cycloaddition with methyl 4-ethynylbenzoate to give the desired compound **3**. Afterwards, reduction of compound **3** with LiAlH$_4$ provided the desired derivative **7**.
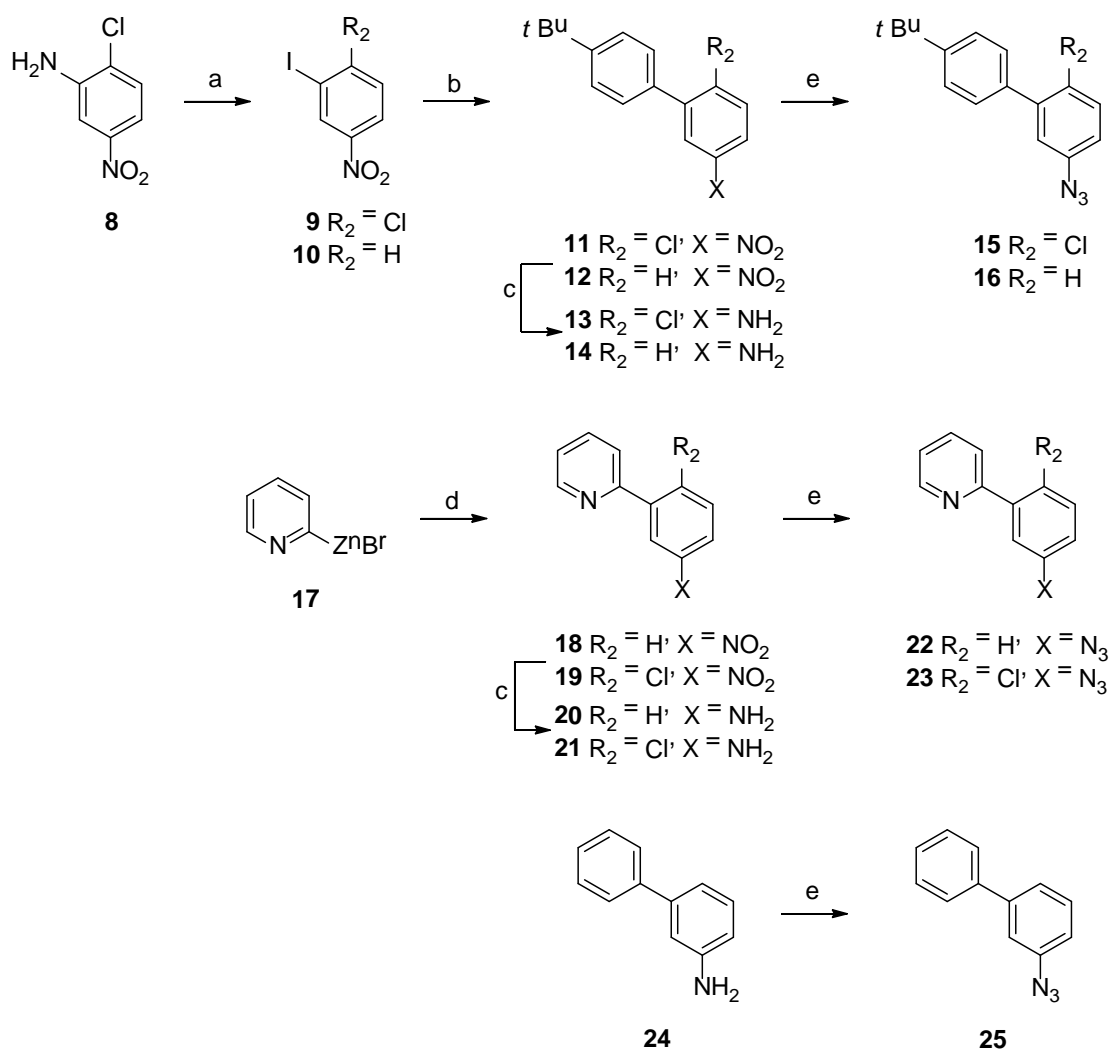
Scheme 2. Reagents and conditions: (a) $NaNO_2$, KI, H_2SO_4, H_2O, 0 ℃ to rt, 1 h; (b) 4-*tert*-Butylphenylboronic acid, $Pd(OAc)_2$, K_2CO_3, $MeOH:H_2O$ (5:1), reflux, 4 h (c) $N_2H_4·H_2O$, $FeCl_3$, active C, MeOH, reflux, 2 h; (d) 1-Iodo-3-nitrobenzene or compound **9**, PPh_3, $Pd(PPh_3)_4$, DMA, THF, 60 ℃; (e) $NaNO_2$, NaN_3, $CH_3COOH:H_2O$ (1:1), 0 ℃ to rt, 2 h.

For the synthesis of analogues **4** and **5** the commercially available 2-pyridylzinc bromide (**17**) was used for the construction of the phenylpyridine moiety. Negishi coupling between compound **17** and 1-iodo-3-nitrobenzene or compound **9** gave the corresponding nitro compounds **18** and **19**. Then, reduction of the nitro group, with hydrazine monohydrate/iron(III) chloride in the presence of active carbon gave the amines **20** and **21**, which were then transformed to the azide derivatives **22** and **23** by the formation of diazonium salt and subsequent reaction with a solution of sodium azide in water. Sharpless cycloaddition between azide **22** and alkyne **32** (Scheme 3) or azide **23** and alkyne **29** (Scheme 3) provided the desired products **4** and **5** respectively.
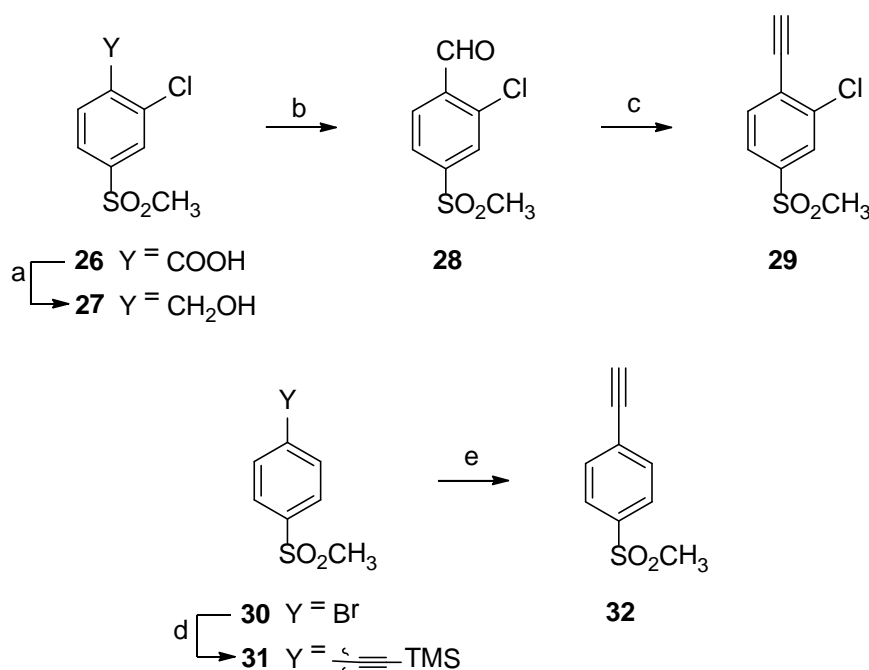
Scheme 3. Reagents and conditions: (a) LiAlH$_4$, THF, 0 °C to rt, 1 h; (b) Dess-Martin periodinane, DCM, rt, 2 h; (c) Bestmann-Ohira reagent, K$_2$CO$_3$, MeOH, 0 °C to rt, 3 h; (d) Trimethylsilylacetylene, CuI, PdCl$_2$(PPh$_3$)$_4$, DCM:Et$_3$N (1:1), rt; (e) TBAF, THF, rt, 1 h.

2.3. Biological Evaluation

We first evaluated the inhibitory effect of selected compounds **1**-**7** on the proliferation of three cancer cell lines [murine leukemia cells (L1210), human T-lymphocyte cells (CEM) and human cervix carcinoma cells (HeLa)] and two endothelial cell lines [human microvascular endothelial cells (HMEC-1) and bovine aortic endothelial cells (BAEC)]. Data are expressed as IC$_{50}$ (50% inhibitory concentration), defined as the concentration at which the compounds reduce cell proliferation by 50% and are shown in Table 1.

Compounds **2** and **4** showed poor activity against tumor cell lines with 50% inhibitory values higher than 100 μM. A modest anti-proliferative activity was observed for compounds **1**, **5** and **7**, with IC$_{50}$ values ≥ 50 μM against the different tumor cell lines. However, these compounds inhibited the proliferation of human microvascular endothelial HMEC-1 cells with IC$_{50}$ values between 10 and 14 μM. Compound **6** proved active in the lower micromolar range in all cell lines tested. The most active compound **3** inhibited tumor and endothelial cell proliferation with IC$_{50}$ values ≤ 1 μM. Thus, although the compounds significantly differ in their inhibitory

activity against different tumor cell lines, they all show pronounced antiproliferative activity against human microvascular endothelial cells.

Table 1. Inhibitory effects of the compounds on cell proliferation (IC_{50}, μM)

	L1210	CEM	HeLa	BAEC	HMEC-1
1	80 ± 29	> 100	57 ± 4	>100	5.6 ± 1.3
2	> 100	> 100	> 100	>100	6.9 ± 4.8
3	1.1 ± 0.0	0.92 ± 0.01	1.1 ± 0.3	0.42 ± 0.04	0.62 ± 0.11
4	> 100	> 100	> 100	> 100	11 ± 1
5	82 ± 72	50 ± 12	> 100	40 ± 10	9.6 ± 0.7
6	10 ± 0	12 ± 1	13 ± 2	7.1 ± 1.5	7.0 ± 1.3
7	95 ± 12	64 ± 4	72 ± 7	>100	11 ± 11
GDC-0499	49 ± 9	58 ± 6	64 ± 4	50 ± 4	41 ± 3

The compounds were also tested for their cytotoxic activity on ovarian cancer cell line (OVCAR5) and two ovarian cancer stem cells (#83, #110), recently isolated.[15] Figure 2 reports the dose-response curve in the three different systems for both Vismodegib (left panel) and compound **4**. Similarly to the data observed for the other cell lines, the cytotoxic activity of the compounds was poor but similar in all the three systems used.
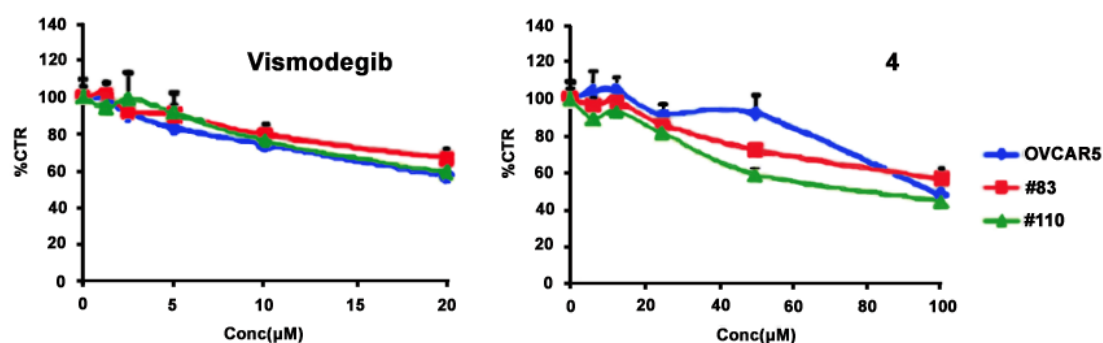

Figure 2. Dose response curves of vismodegib and compound **4** in #83, #110 and OVCAR5 cell lines. Data are expressed as % of controls and are the mean of two experiments done in sixplicates.

Glioblastoma is the most common and lethal primary brain tumour. Despite surgical removal and aggressive chemo/radiotherapy, its prognosis remains hitherto very poor. Hedgehog signalling plays a central role in glioblastoma development and progression.[16] For this reason, we used two glioblastoma cell lines, U251 and SF268, in order to evaluate the efficacy of the described compounds against this type of cancer. To this end, we cultured U251 and SF268 cells until semi-confluent and then

added the described compounds at 25 μM. Cells were collected after 48h. BrdU was added in the medium at 0.4 mg/ml for the last 1 hour. As illustrated in Figure 3a, the compounds **2–7** significantly reduced cell proliferation (from 20 to 83%), although only compounds **3** and **6** at the levels of Vismodegib. The effect was similar in both cell lines, but more pronounced in U251 cells. We also estimated the effect of the compounds on cell death, and we analysed by flow cytometry apoptosis, using active caspase-3 immunofluorescence. Vismodegib and compound **3** induced cell death in both cell lines, while compounds **1**, **6** and **7** induced low levels of apoptosis mainly in U251 cells (Figure 3b). We then selected the compounds that showed significant effect in terms of both proliferation and apoptosis, and the U251 cell line that proved more sensitive, and assessed the dose response of those cells to compound concentrations from 1 to 50 μM (Figure 3c, d). Our results showed a clear dose-dependent response for both proliferation inhibition and apoptosis against all the compounds tested, with compound **3** and Vismodegib having the more prominent and very similar effect.
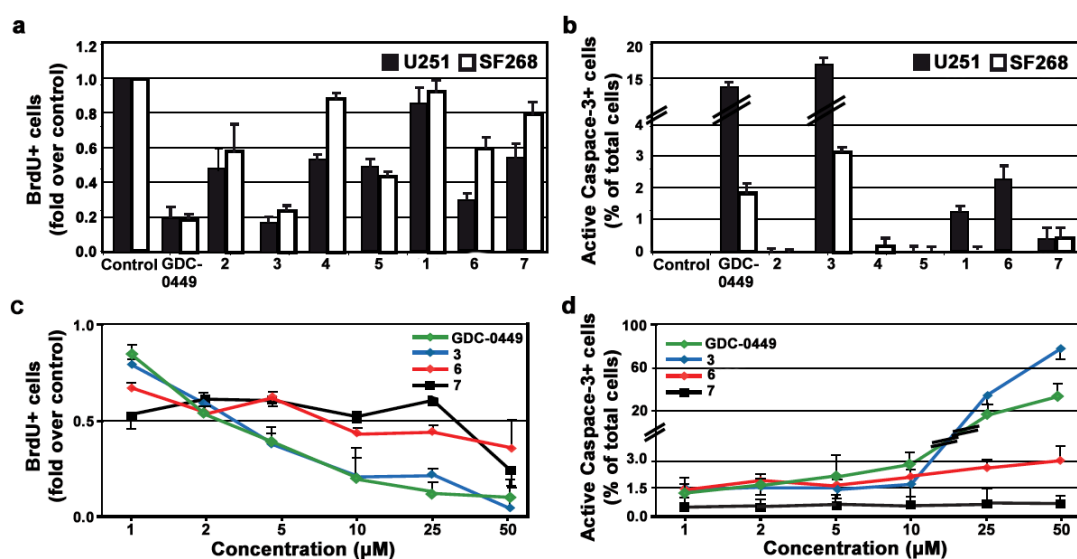

Figure 3. a. Effect of the described compounds on the proliferation of U251 and SF268 glioblastoma cell lines, at a concentration of 25μM after 48h of culture, as estimated by BrdU incorporation and analysis by flow cytometry. Results are presented as fold over the proliferation of control cultures where only the vehicle was added. **b.** Effect of the described compounds on apoptosis of U251 and SF268 cells, at a concentration of 25μM after 48h of culture, as estimated by flow cytometry detecting active Caspase-3 expression. **c, d.** Dose response curves of the effect of Vismodegib, **3**, **6** and **7** on the proliferation (c) and apoptosis (d) of U251 cells, after 48h of culture. Mean of 3 independent experiments is shown. Values are expressed as mean±SD.

Given the cell cycle arrest shown by the BrdU-incorporation analysis, we sought to investigate whether there is a specific checkpoint activated by the different compounds. We thus performed cell cycle analysis, using propidium iodide.

Interestingly, U251 cells exposed to Vismodegib or compound **3** (Figure 4) accumulate in the S phase of the cell cycle. However, this does not reflect higher proliferation of those cells, since the BrdU incorporation assay clearly showed that these two compounds severely impaired cell proliferation. Consequently, we can assume that exposure to Vismodegib or compound **3** activates an intra-S checkpoint in those cells.
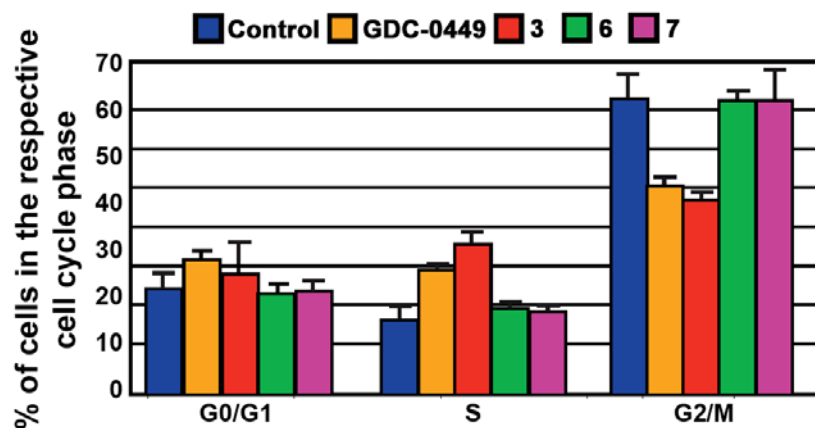

Figure 4. Effect of the described compounds on the cell cycle of U251 cells, at a concentration of 25μM after 48h of culture, as estimated by flow cytometry using Propidium Iodide. Apoptotic and aneuploid cells have been excluded. Mean of 3 independent experiments is shown. Values are expressed as mean±SD.

In order to investigate whether the effect of the compounds tested is indeed mediated by inhibition of the Hedgehog pathway, we performed transcriptional analysis by quantitative RT-PCR for the main genes of the Hh pathway, Gli1, Gli2 and Ptch1. Surprisingly, while Vismodegib addition did result in significant reduction of the transcriptional levels of all 3 genes tested, compound **3** did not have a significant effect in Hh pathway, showing that this compound mediates proliferation inhibition and cell death via another mechanism that would be interesting to be tested in the future. In contrast, compound **6**, although having a milder effect on proliferation and apoptosis in the cell lines tested, mediated this effect, at least partly, via Hh pathway inhibition (Figure 5).
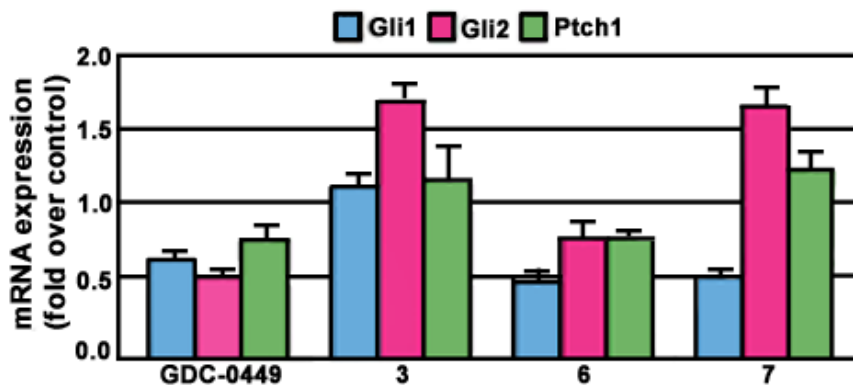
Figure 5. Transcriptional analysis of components of the Hedgehog signaling pathway as estimated by quantitative RT-PCR, 24h upon addition of the described compounds at 25μM. Results are expressed as fold change over the mRNA expression in the control cultures, where only the vehicle was added. Mean of 3 independent experiments is shown. Values are expressed as mean±SD.

The activity of compound **3** against endothelial cells moved us to evaluate its effect on endothelial cell migration and tube formation, two important processes involved in the formation of new blood vessels. Compound **3** did not inhibit endothelial cell migration (not shown), but a dose-dependent inhibition of tube formation was observed (Figure 6).
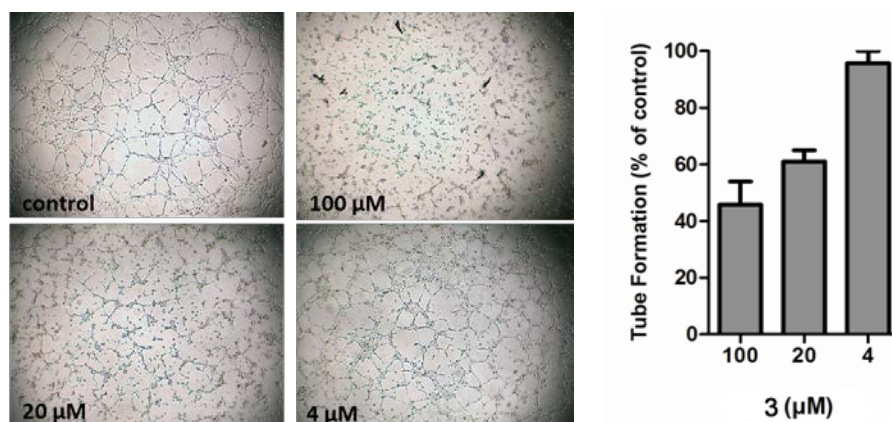

Figure 6. Effect of compound **3** on angiogenesis. HMEC-1 cells were seeded on matrigel in the presence of different concentrations (100 – 20 – 4 µM) of compound **3**. After 3 h of incubation, endothelial cell tubes were photographed and scored. Average and S.E.M (n=4) are shown.*p<0.05.

3. Conclusions

The preparation of seven 1,4-diphenyl-1,2,3-triazole derivatives has been described by Huisgen cycloaddition. Molecular modeling results suggest the replacement of the amide moiety of Vismodegib with triazole group as a possibility for further structure-based optimization studies. The biological evaluation on different types of cell lines showed interesting activity of compounds **3** and **6** against cancer and endothelial cells.

Compound **3** showed interesting activity on glioblastoma cells and seems to block cells in S phase similarly to Vismodegib. Transcriptional analysis by quantitative RP-PCR for the main genes of the Hh pathway, Gli1, Gli2 and Ptch1 confirmed compound **6** as able to interact with Hh pathway and suggested a different mechanism for compound **3** to justify its ability to inhibit proliferation. Moreover, compound **3** proved to be a potential inhibitor of the formation of blood vessels. To sum up, all the reported results point out the subsequent: a) 1,4-diphenyl-1,2,3-triazole framework as a good scaffold for the generation of new promising compounds and b) the use of 1,2,3-triazole system as a useful way to connect pharmacophores.

4. Experimental

4.1. General procedures (*see Supporting Information*)

4.2. Synthesis (*see Supporting Information*)

4.3. Molecular modeling

The tridimensional structure of SMO in complex with a small molecule antagonist was downloaded from the Protein Data Bank (www.rcsb.org/pdb; PDB accession code: 4JKV).[11] Co-crystalized ligands and water molecules were manually removed, and the receptor was prepared for docking with the *make_receptor* utility of the OEDocking software from OpenEye.[12, 13] Ligand conformational analysis was performed with the software OMEGA, which generated up to 600 conformers for each ligand.[17-19] Molecular docking was performed with HYBRID from OpenEye,[12, 13] using the "High" docking resolution flag and all other default options, while rescoring was performed by means of the XSCORE function.[14]

4.4. Biological evaluation

4.4.1. Cell lines.

Endothelial cells: Bovine aortic endothelial cells (BAEC) and human dermal microvascular endothelial cells (HMEC-1) were seeded in 48-well plates at 10,000 cells/well and 20,000/well, respectively. After 24 h, 5-fold dilutions of the compounds were added. The cells were allowed to proliferate 3 days (or 4 days for HMEC-1) in

the presence of the compounds, trypsinized, and counted by means of a Coulter counter (Analis, Belgium).

Tumor cells: Human cervical carcinoma (HeLa) cells were seeded in 96-well plates at 15,000 cells/well in the presence of different concentrations of the compounds. After 4 days of incubation, the cells were trypsinized and counted in a Coulter counter. Suspension cells (Mouse leukemia L1210 and human lymphoid Cem cells) were seeded in 96-well plates at 60,000 cells/well in the presence of different concentrations of the compounds. L1210 and Cem cells were allowed to proliferate for 48 h or 96 h, respectively and then counted in a Coulter counter. The 50% inhibitory concentration (IC_{50}) was defined as the compound concentration required to reduce cell proliferation by 50%.

The glioblastoma cell line U251 (ECACC) was cultured in EMEM, supplemented with 2mM Glutamine, 1% Non Essential Amino Acids, 1mM Sodium Pyruvate and 10% Foetal Bovine Serum (all by Life Technologies). Glioblastoma SF268 cells were cultured in RPMI (Life Technologies), supplemented with 2mM Glutamine and 10% Foetal Bovine Serum.

#83 and #110 cell lines were obtained and maintained as already reported.[15] Briefly they were maintained in low adherence flasks (Corning) under stem-cell conditions: serum-free DMEM/F12 supplemented with 5 µg/mL insulin (Sigma), 20 ng/mL human recombinant epidermal growth factor (EGF, Peprotech), 10 ng/mL basic fibroblastic growth factor (bFGF, Peprotech) and B27 Supplement (Gibco). For cytotoxic experiments, Ovcar5 and #83 and #110 cells derived from dissociated spheres were plated in 96 well plates at a concentration of 12500 cells/mL. 96 hours later cells were treated with different drugs doses. Cell survival was assessed at 72 h by MTS assay and dose-response curves were plotted.

4.4.2. Tube formation assay.

Wells of a 96-well plate were coated with 70 µl matrigel (10 mg/ml, BD Biosciences, Heidelberg, Germany) at 4°C. After gelatinization at 37°C during 30 min, HMEC-1 cells were seeded at 60,000 cells/well on top of the matrigel in 200 µl DMEM containing 10% FCS and the test compounds. After 3 hours of incubation, the cell structures were photographed and scored. A two-tailed unpaired Student's *t*-test was used to assess the significance of the obtained results.

4.4.3. Flow cytometry.

BrdU was detected using the BrdU Flow Kit and anti-BrdU conjugated with FITC (at 1/50). Active caspase-3 was detected using PE-conjugated anti-active Caspase 3 antibody (1/25) and BD Perm/Wash reagent (all by BD Biosciences). Cell cycle analysis was performed using propidium iodide. Briefly, cells were permeabilised with ethanol on ice and stained for 40 min at $37^{o}C$ with 50 μg/ml propidium iodide in the presence of 0.1 mg/ml RNase A and 0.05% Triton X-100 (all from Sigma-Aldrich). FACS analysis was performed using LSR Fortessa and FACS DiVa software (BD Biosciences).

4.4.4. Reverse transcription and quantitative RT-PCR.

RNA extraction was performed using Absolutely RNA Microprep kit (Stratagene). 1 μg of purified RNA was used to synthesize the first strand cDNA in a final volume of 50 μl, using a Superscript II (Invitrogen) and random hexamers (Roche). qPCR analyses were performed with one-hundredth of the cDNA reaction as template, using a Quantifast SYBR Green mix (Qiagen) on an Agilent Technologies Stratagene Mx3500P real-time PCR system. Hypoxanthine phosphoribosyltransferase (HPRT) and βeta-actin were used as housekeeping internal reference genes. All primers were designed to amplify amplicons in the intron-exon junctions. Specificity of the PCR amplification was assessed by electrophoresis of the amplicons on 2% agarose gels.

References:

[1] A. E. Proctor, L. A. Thompson, C. L. O'Bryant, *Ann. Pharmacot.* **2014**, *48*, 99-106.

[2] J. M. Y. Ng, T. Curran, *Nature Rev. Cancer* **2011**, *11*, 493-501.

[3] T. Brinkhuizen, M. G. Reinders, M. van Geel, A. J. L. Hendriksen, A. D. C. Paulussen, V. J. Winnepenninckx, K. B. Keymeulen, P. M. M. B. Soetekouw, M. M. van Steensel, K. Mosterd, *J. Am. Acad. Derm.* **2014**, *71*, 1005-1008.

[4] P. Heretsch, L. Tzagkaroulaki, A. Giannis, *Bioorg. Med. Chem.* **2010**, *18*, 6613-6624.

[5] P. A. Sotiropoulou, M. S. Christodoulou, A. Silvani, C. Herold-Mende, D. Passarella, *Drug Discov. Today* **2014**, *19*, 1547-1562.

[6] P. Infante, M. Mori, R. Alfonsi, F. Ghirga, F. Aiello, S. Toscano, C. Ingallina, M. Siler, D. Cucchi, A. Po, E. Miele, D. D'Amico, G. Canettieri, E. De Smaele, E. Ferretti, I. Screpanti, G. Uccello Barretta, M. Botta, B. Botta, A. Gulino, L. Di Marcotullio, *The EMBO Journal* **2014**, DOI: 10.15252/embj.201489213.

[7] F. Arioli, S. Borrelli, F. Colombo, F. Falchi, I. Filippi, E. Crespan, A. Naldini, G. Scalia, A. Silvani, G. Maga, F. Carraro, M. Botta, D. Passarella, *ChemMedChem* **2011**, *6*, 2009-2018.

[8] F. Colombo, C. Tintori, A. Furlan, S. Borrelli, M. S. Christodoulou, R. Dono, F. Maina, M. Botta, M. Amod, J. Bosch, D. Passarella, *Bioorg. Med. Chem. Lett.* **2012**, *22*, 4693-4696.

[9] V. V. Rostovtsev, L. G. Green, V. V. Fokin, K. B. Sharpless, *Angew. Chem. Int. Ed.* **2002**, *114*, 2708-2711.

[10] M. Mori, G. Vignaroli, Y. Cau, J. Dinić, R. Hill, M. Rossi, D. Colecchia, M. Pešić, W. Link, M. Chiariello, C. Ottmann, M. Botta, *ChemMedChem* **2014**, *9*, 973-983.

[11] C. Wang, H. Wu, V. Katritch, G. W. Han, X. P. Huang, W. Liu, F. Y. Siu, B. L. Roth, V. Cherezov, R. C. Stevens, *Nature* **2013**, *16*, 338-343.

[12] OEDocking version 3.0.0, OpenEye Scientific Software, Santa Fe, NM. http://www.eyesopen.com

[13] M. McGann, *J. Chem. Inf. Model.* **2011**, *51*, 578-596.

[14] R. Wang, L. Lai, S. Wang, *J. Comput.-Aided Mol. Des.* **2002**, *16*, 11-26.

[15] F. Ricci, S. Bernasconi, P. Perego, M. Ganzinelli, G. Russo, F. Bono, C. Mangioni, R. Fruscio, M. Signorelli, M. Broggini, G. Damia, *Cell Cycle* **2012**, *10*, 1966-1976.

[16] S. Tanaka, D. N. Louis, W. T. Curry, T. T. Batchelor, J. Dietrich, *Nat. Rev. Clin. Onc.* **2013**, *10*, 14-26.

[17] OMEGA version 2.4.6, OpenEye Scientific Software, Santa Fe, NM. http://www.eyesopen.com.

[18] P. C. D. Hawkins, A. G. Skillman, G. L. Warren, B. A. Ellingson, M. T. Stahl, *J. Chem. Inf. Model.* **2010**, *50*, 572-584.

[19] P. C. D. Hawkins, A. Nicholls, *J. Chem. Inf. Model.* **2012**, *52*, 2919-2936.